Supplementary Material (ESI) for Dalton Transactions

Encapsulation of discrete $(H_2O)_{12}$ clusters in a 3-D three-fold interpenetrating metal-organic framework host with (3,4)-connected topology

Xiuli Wang,* Hongyan Lin, Bao Mu, Aixiang Tian and Guocheng Liu

[a] *Faculty of Chemistry and Chemical Engineering, Bohai University, Jinzhou, 121000, P.R. China*

ELECTRONIC SUPPLEMENTARY INFORMATION

Experimental Section

Materials and instrumentation

Ligand **L** was synthesized by the literature method.[1] H_3BTC was commercially obtained from Aldrich and used without further purification. All other reagents were of reagent grade. FT-IR spectra (KBr pellets) were taken on a Magna FT-IR 560 spectrometer and the elemental analyses (C, H, and N) were carried out on a Perkin-Elmer 2400C elemental analyzer. Powder XRD investigations were carried out on a Bruker AXS D8-Advanced diffractometer at 40 kV, 40 mA with Cu Kα (λ =1.5406 Å) radiation. The electrochemical experiments were carried out using a CHI 440 Electrochemical Quartz Crystal Microbalance. A conventional three-electrode cell was used at room temperature. The modified electrode was used as working electrode. A SCE and a platinum wire were used as reference and auxiliary electrodes, respectively.

Preparation of the title complex **1** modified carbon paste electrode (**1**-CPE): The **1**-CPE was fabricated as follows: 0.25 g graphite powder and 0.015 g complex **1** were mixed and ground together by agate mortar and pestle for approximately 20 min to achieve an even, dry mixture; to the mixture 0.08 ml paraffin oil was added and stirred with a glass rod; then the homogenized mixture was used to pack 2 mm inner diameter glass tubes to a length of 0.5 cm. The electrical contact was established with the copper stick, and the surface of the **1**-CPE was wiped with weighing paper. The same procedure was used for preparation of bare CPE without title complex.

Crystallographic data for **1** was collected at 293(2) K on a Bruker Smart 1000 CCD diffractometer with Mo Kα (λ = 0.71073 Å) by ω scan mode. The structure was solved by direct methods using the SHELXS program of the SHELXTL package and refined by full-matrix least-squares methods with SHELXL. Metal atoms in the complex were located from the *E*-maps, and other non-hydrogen atoms were located from successive difference Fourier maps and refined with anisotropic thermal parameters on F^2. The hydrogen atoms of the ligand were generated theoretically onto the specific atoms and refined isotropically with fixed thermal factors.

1 M. Sarkar and K. Biradha, *Cryst. Growth. Des*, 2006, **6**, 202.

A summary of crystal data and structure refinement for complex **1** is provided in **Table S1**. Selected bond lengths and angles are listed in **Table S2**. Crystallographic data (excluding structure factors) for the structure reported in this paper have been deposited with the Cambridge Crystallographic Data Center as supplementary publication number CCDC 724742.

Table S1. Crystal data and structure refinement summary for complex **1**

Empirical formula	$C_{72}H_{56}Cu_3N_{12}O_{22}$
Formula weight	1631.91
Temperature (K)	150(2)
Crystal system	Trigonal
Space group	R-3
a (Å)	18.5636(3)
b (Å)	18.5636(3)
c (Å)	19.7224(6)
α (◦)	90
β (◦)	90
γ (◦)	120
Volume (Å ^{3})	5885.9(2)
Z	9
D_{calc} (g/cm^3)	1.381
Absorption coefficient (mm^{-1})	0.884
F(000)	2504
Crystal size (mm)	0.14 x 0.10 x 0.07
θ range (◦)	1.63–24.97
Range of *h*, *k*, *l*	-22/22, -22/22, -23/23
Reflections collected	18822
Independent reflections	2299 (R_{int} = 0.0446)
Data / restraints / parameters	2299 / 0 / 178
Goodness-of-fit on F^2	1.181
Final *R* indices [$I > 2\sigma(I)$]	R^a= 0.0348, wR^b= 0.0992
R indices (all data)	R^a= 0.0430, wR^b= 0.1143
Largest diff. peak and hole (e Å $^{-3}$)	0.831 and -0.312

$^a R_1 = \Sigma||F_0|-|F_c||/\Sigma|F_0|$; $^b wR_2 = \Sigma[w(F_0^2-F_c^2)^2]/\Sigma[w(F_0^2)^2]^{1/2}$.

Table S2. Selected bond distances (Å) and angles (deg) for complex **1**

Cu(1)–O(1)	1.9263(17)	Cu(1)–O(1)#1	1.9263(17)
Cu(1)–N(1)	2.013(2)	Cu(1)–N(1)#1	2.012(2)
O(1)#1–Cu(1)–O(1)	180.00(2)	O(1)#1–Cu(1)–N(1)#1	90.08(8)
O(1)–Cu(1)–N(1)#1	89.92(8)	O(1)#1–Cu(1)–N(1)	89.92(8)
O(1)–Cu(1)–N(1)	90.08(8)	N(1)#1–Cu(1)–N(1)	180.00(2)

Symmetry code for #1: -x+1,-y,-z+1.

Table S3. Hydrogen-bonded geometry (Å, °) for complex **1**

D–H···A	D–H	H···A	D···A	D–H···A
O(2W)–H (2WB)··· O (2W)[a]	0.85(2)	2.01(2)	2.85(3)	174(10)
O(1W)–H (1WB)··· O (1W)[b]	0.85(2)	2.15(2)	2.57(2)	110(10)
O(2W)–H (2WA)··· O (1W)[c]	0.85(2)	2.16(2)	2.96(2)	158(9)

Symmetry code for (a) -2/3+x,-1/3+y,-4/3+z (b) -1/3+x-y,-2/3+x,1/3-z (c) 1/3-y,-1/3+x-y,-4/3+z.

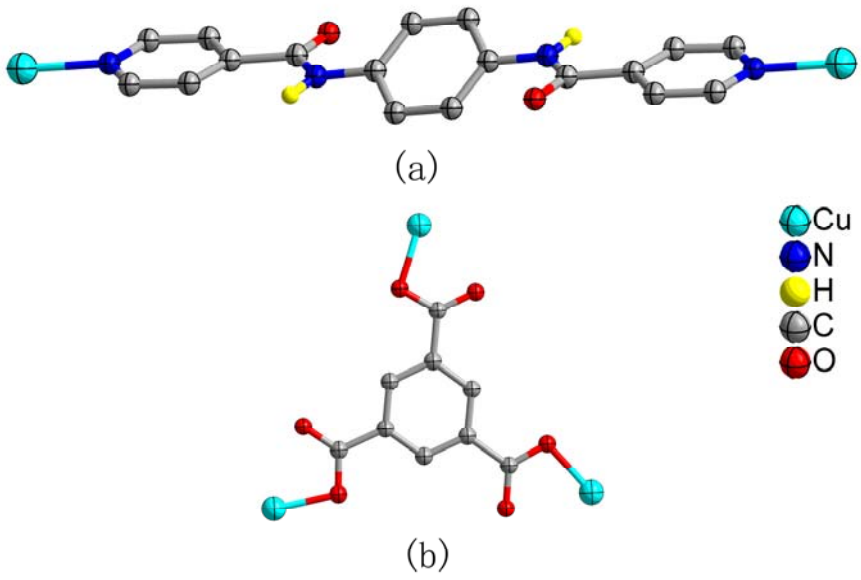

Fig. S1. Coordination mode of **L** ligand and BTC ligand.

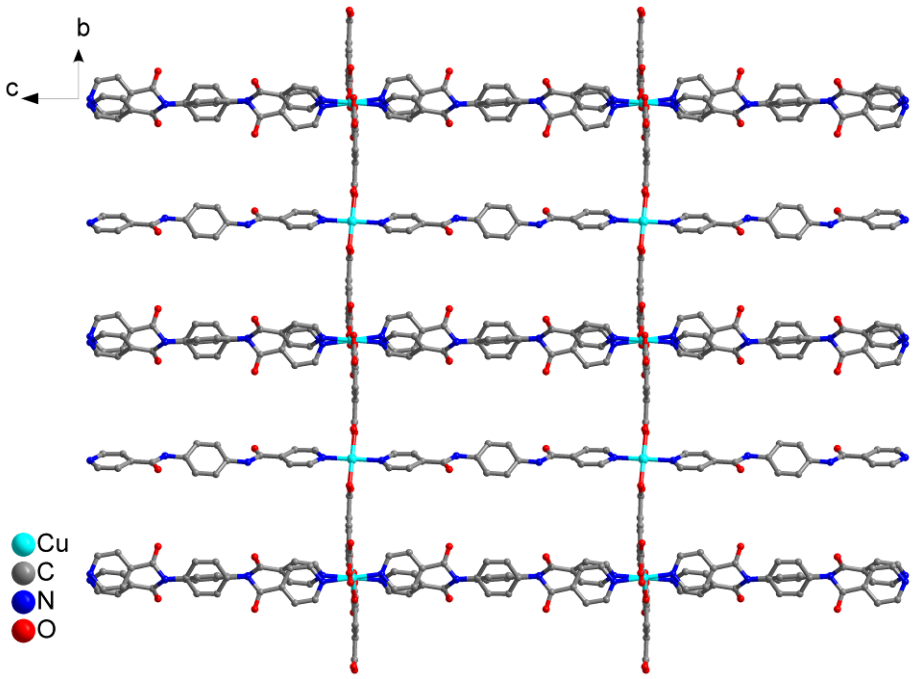

(a)

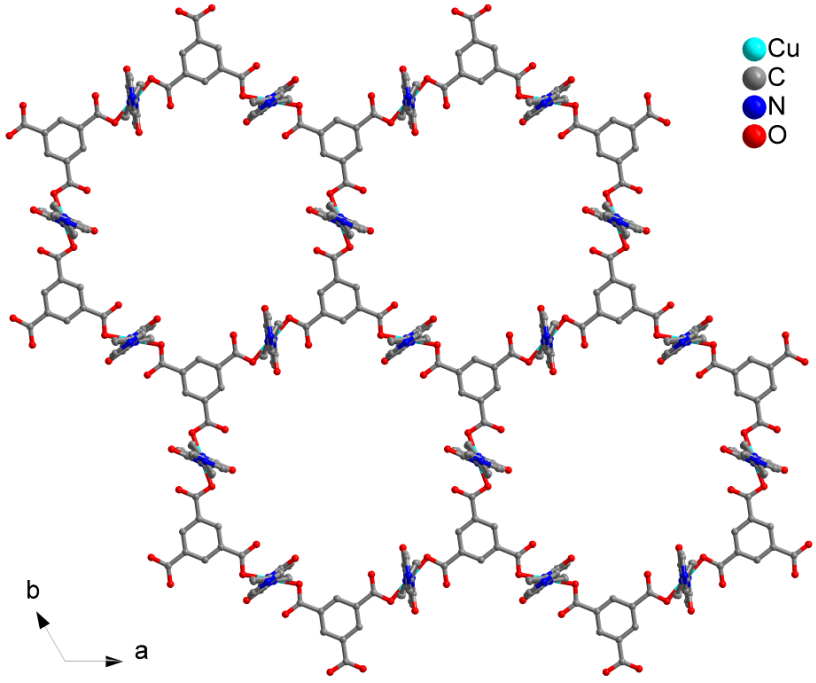

(b)

Fig. S2. Ball-and-stick representation of the 3-D metal-organic framework of complex **1:** along a-axis (a) and along c-axis (b). All H atoms and lattice water molecules have been omitted for clarity.

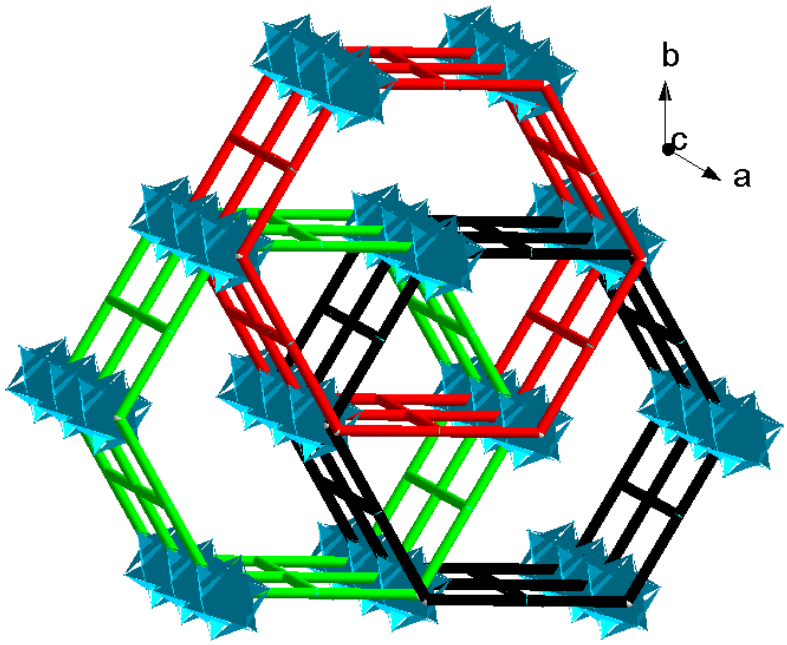

Fig. S3. View of three-fold interpenetrating 3D metal-organic framework in **1** along the c-axis. Stick representation of the hexagon-like channels based on 3D metal-organic framework $[Cu_3(L)_3(BTC)_2]_{3n}$, encapsulating $(H_2O)_{12}$ water clusters shown in a polyhedral representation.

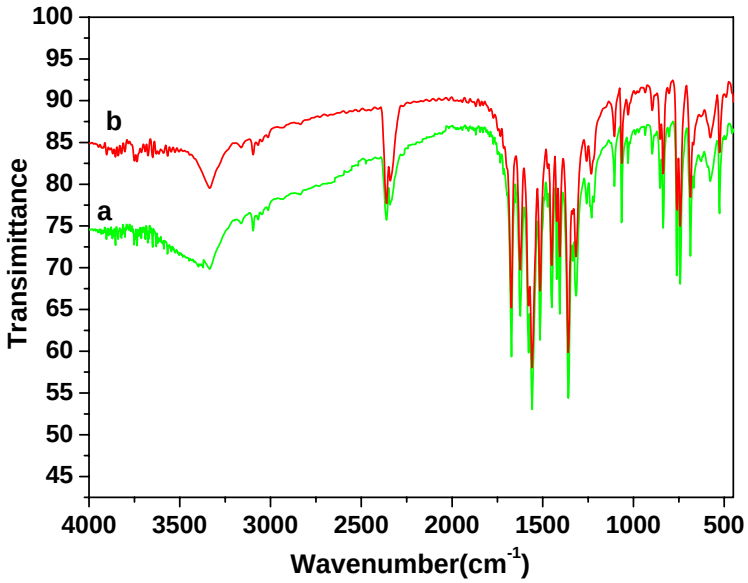

Fig. S4. The IR spectra of complex **1.** (a) Crystal sample containing water clusters, (b) Crystal sample without water clusters.

The FT-IR spectra of complex **1** show a strong band with two peaks at around 3396 and 3325 cm^{-1} (curve a), which should be assigned to the vibrations of hydroxyl groups. When the solid samples were heated in vacuum at 200 °C for 2 h, the peak at 3396 cm^{-1} vanished (curve b). As reported, the stretching vibrations of O–H are found to be size specific, spreading over a wide range from 3720 to 2935 cm^{-1}, with the larger nuclear clusters exhibiting the O–H vibration below 3400 cm^{-1} and which shifts with increasing ring size to smaller values.[2] Therefore, the peak at 3396 cm^{-1} in the IR spectra can be regarded as the O–H vibration in the water clusters with six-membered rings and its vanishing can be attributed to the lose of water molecules.

The IR spectra display the typical stretching bands of carboxylate groups between 1300 and 1660 cm^{-1}, a very strong band appears at around 1625 cm^{-1} due to the asymmetric stretching (ν_{as}) of the carboxylate group; the symmetrical stretching (ν_s) band of this group appears at 1480–1670 and 1350–1455 cm^{-1}, respectively.[3] No strong absorption peaks around 1700 cm^{-1} for –COOH are observed, indicating that carboxyl groups of organic moieties in **1** are completely deprotonated.[3] The bands at about 1556, 1480, 1064, and 705 cm^{-1} may be attributed to the ν_{C-N} stretching of the pyridyl ring. Weak absorptions observed at 3010–3170 cm^{-1} for **1** can be attributed to the ν_{C-H} stretching bands.

2 (a) M. Mascal, L. Infantes and J. Chisholm, *Angew. Chem., Int. Ed.*, 2006, **45**, 32; (b) J. W. Shin, N. I. Hammer, E. G. Diken, M. A. Johnson, R. S. Walters, T. D. Jaeger, M. A. Duncan, R. A. Christie and K. D. Jordan, *Science*, 2004, **304**, 1137.

3 (a) S. N. Wang, J. F. Bai, H. Xing, Y. Z. Li, Y. Song, Y. Pan, M. Scheer, X. Z. You, *Cryst. Growth. Des.*, 2007, **7**, 745; (b) A. H. Yang, H. Zhang, H. L. Gao, W. Q. Zhang, L. He, J. Z. Cui, *Cryst. Growth. Des.*, 2008, **8**, 3354.

4 (a) X. J. Gu and D. F. Xue, *Cryst. Growth. Des*., 2006, **6,** 2551; (b) L. J. Bellamy, The Infrared Spectra of Complex Molecules; Wiley, New York, 1958.

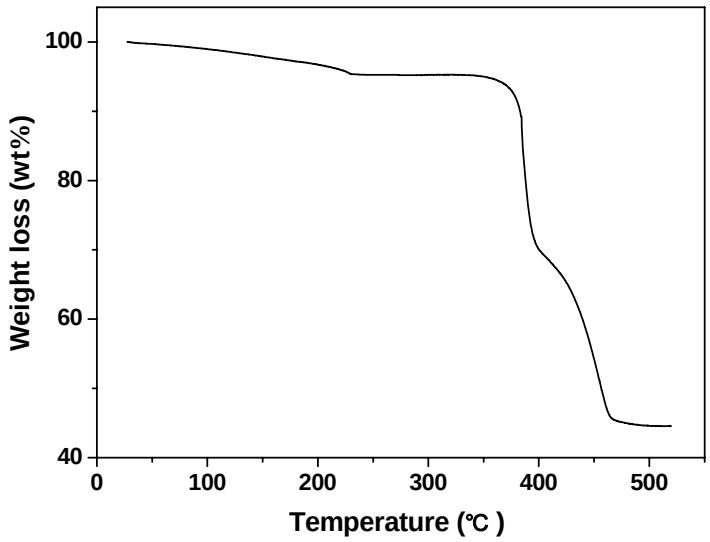

Fig. S5 TG curve for complex **1.**

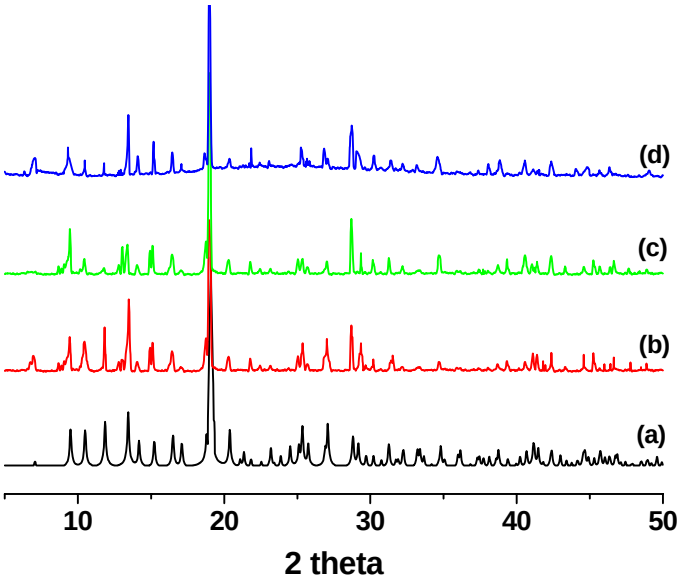

Fig. S6 XRD patterns: (a) simulated from single-crystal X-ray data; (b) as-synthesized complex **$[Cu_3(L)_3(BTC)_2]_3$·~12H_2O (1);** (c) taken after heating at 200 °C under vacuum for 2 h; (d) after rehydration of sample for 24 h.

The powder X-ray diffraction pattern of an as-synthesized crystal of **1** was almost identical to that calculated from the single-crystal structure. The XRD of crystals **1** heated to 200 °C under vacuum for 2 h revealed that lattice water molecules in the structure were completely removed and the chemical composition of the powder is **$[Cu_3(L)_3(BTC)_2]_3$**. When the sample **1** was immersed in water for 24 h, the original framework is recovered as indicated by the similar XRD curve to that of the fresh one.

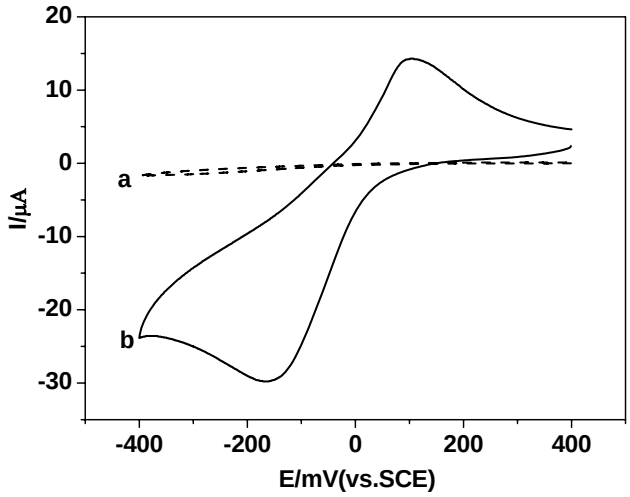

Fig. S7. Cyclic voltammograms of (a) the bare CPE and (b) **1**-CPE in 0.1 M pH 2.5 phosphates buffer solution in the potential range of 400 – -400 mV. Scan rate: 50 mVs^{-1}.

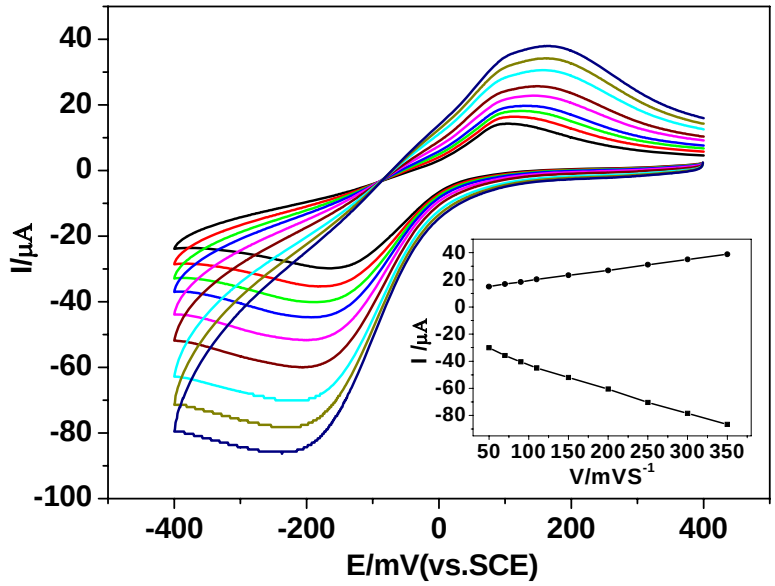

Fig. S8. Cyclic voltammograms of **1**-CPE in pH 2.5 phosphate buffer solution at different scan rates (from inner to outer) 50, 70, 90, 110, 150, 200, 250, 300, and 350 mV s^{-1} of **1**-CPE. The inset shows the plots of the anodic and the cathodic peak currents *vs.* scan rates.

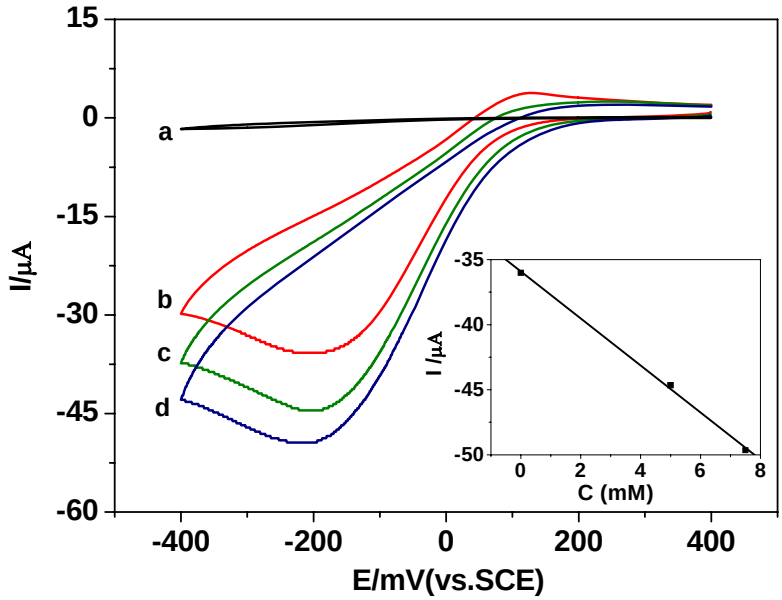

Fig. S9. Cyclic voltammograms of a bare CPE in phosphate buffer solution with pH of 2 containing 5 mM $NaNO_2$ (a) and **1**-CPE in phosphate buffer solution containing NO_2^- concentrations of 0.0 (b), 5.0 (c) and 7.5 (d) mM. Scan rate: 50 mVs^{-1}. Inset: the variation of cathodic peak currents *vs.* nitrite concentrations.